Climatic Change (2009) 94:275–286
DOI 10.1007/s10584-008-9515-9

Global cooling: increasing world-wide urban albedos to offset CO_2

Hashem Akbari · Surabi Menon · Arthur Rosenfeld

Received: 29 January 2008 / Accepted: 4 September 2008 / Published online: 20 November 2008

Abstract Increasing urban albedo can reduce summertime temperatures, resulting in better air quality and savings from reduced air-conditioning costs. In addition, increasing urban albedo can result in less absorption of incoming solar radiation by the surface-troposphere system, countering to some extent the global scale effects of increasing greenhouse gas concentrations. Pavements and roofs typically constitute over 60% of urban surfaces (roof 20–25%, pavements about 40%). Using reflective materials, both roof and pavement albedos can be increased by about 0.25 and 0.15, respectively, resulting in a net albedo increase for urban areas of about 0.1. On a global basis, we estimate that increasing the world-wide albedos of urban roofs and paved surfaces will induce a negative radiative forcing on the earth equivalent to offsetting about 44 Gt of CO_2 emissions. At ~\$25/tonne of CO_2, a 44 Gt CO_2 emission offset from changing the albedo of roofs and paved surfaces is worth about \$1,100 billion. Furthermore, many studies have demonstrated reductions of more than 20% in cooling costs for buildings whose rooftop albedo has been increased from 10–20% to about 60% (in the US, potential savings exceed \$1 billion per year). Our estimated CO_2 offsets from albedo modifications are dependent on assumptions used in this study, but nevertheless demonstrate remarkable global cooling potentials that may be obtained from cooler roofs and pavements.

1 Introduction

In many urban areas, pavements and roofs constitute over 60% of urban surfaces (see Table 1; roof 20–25%, pavements about 40%) (Akbari et al. 2003; Rose et al.

H. Akbari (✉) · S. Menon
Lawrence Berkeley National Laboratory, Berkeley, CA, USA
e-mail: H_Akbari@lbl.gov

A. Rosenfeld
California Energy Commission, Sacramento, CA, USA
e-mail: Arosenfe@energy.state.ca.us

Table 1 Urban fabric

Metropolitan Areas	Vegetation	Roofs	Pavements	Other
Salt Lake City	33.3	21.9	36.4	8.5
Sacramento	20.3	19.7	44.5	15.4
Chicago	26.7	24.8	37.1	11.4
Houston	37.1	21.3	29.2	12.4

Source: Rose et al. (2003)

2003; Akbari and Rose 2001a, b). Many studies have demonstrated buildings cooling-energy savings in excess of 20% upon raising roof reflectivity from an existing 10–20% to about 60%. We estimate a U.S. potential savings in excess of $1 billion per year in net annual energy bills (cooling-energy savings minus heating-energy penalties). Increasing the albedo of urban surfaces (roofs and pavements) can reduce the summertime urban temperature and improve the urban air quality (Taha 2001, 2002; Taha et al. 2000; Rosenfeld et al. 1998; Akbari et al. 2001; Pomerantz et al. 1999). The energy and air-quality savings resulting from increasing urban surface abedos in the U.S. alone can exceed $2 billion per year.

Increasing the urban albedo results in reflecting more of the incoming global solar radiation and countering to some extent the effects of global warming. Here we quantify the effect of increasing the albedo of urban areas on in terms of CO_2 emission offset.

2 Estimating global urban areas

Figure 1 lists the area densities for the 100 largest metropolitan areas of the world (Demographia 2007). The median area density is about 430 m^2 per urban dweller. The 100 largest metropolitan areas (with a total population of 670 million) comprise about 0.26% of the Earth land area. Assuming that about 3 billion people live in urban areas, the total urban area of the globe is estimated at about 1.2% of the land area.

As an independent verification for the estimate of urban areas, we used the data from Global Rural–Urban Mapping Project (GRUMP) Urban Extent Mask (CIESIN 2007). The Urban Extent Mask combines National Oceanic and Atmospheric Administration measurements of nighttime lights with the US Defence Mapping Agency Digital Chart of the World's Populated Places to assess the geographic extents of rural and urban areas (Balk et al. 2004). Equal-area sinusoidal projection of the 30-arc-sec urban extent mask indicates that of the Earth's 149 million km^2 of land area, 128 million km^2 is rural and 3.5 million km^2 is urban. The 3.5 million km^2 of urban land represents 2.4% of global land area and 0.7% of global surface area. Most of the 17.5 million $km^2$of unclassified land lies in Antarctica (14 million km^2) or Greenland (2.2 million km^2). The GRUMP estimate of 2.4% is twice the estimate of 1.2%.[1] Furthermore, the analysis from McGranahan et al. (2005) shows that the urban areas account for 2.8% of the land area. We expect that the GRUMP estimate is closer to reality, since the population densities in the world's

[1]We note that a United States Geological Survey analysis of 1992 data shows a value of 0.17% for the fraction of the urban areas to the total land surface area (USGS 1999). This number is seven to 16 times smaller than the other three estimates shown above.

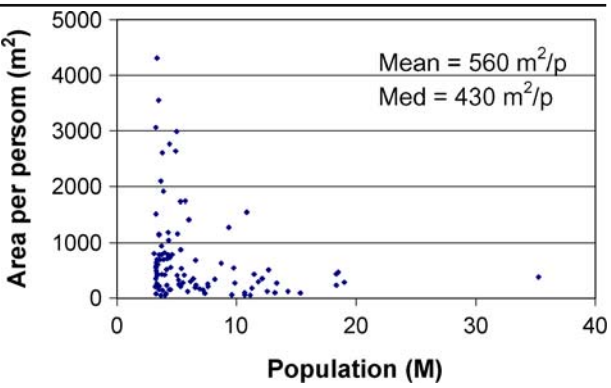

Fig. 1 Area density for the 100 largest cities in the world; 670 million people live in these cities. Source: Demographia (2007)

100 largest cities are probably higher than in other urban areas. In our calculations, we conservatively assume that urban areas are 1% of the land area.

3 Potentials for urban albedo change

Rose et al. (2003) have estimated the fractions of the roof and paved surface areas in four U.S. cities. The fraction of roof areas in these four cities varies from 20% for less dense cities to 25% for more dense cities. The fraction of paved surface areas varies from 29% to 44%. Many metropolitan urban areas around the world are less vegetated than typical U.S. cities. For this analysis, we consider an average area fraction of 25% and 35% for roof and paved surfaces, respectively.

Akbari and Konopacki (2005) have reviewed the solar reflectance of typical roofing materials used on residential and commercial buildings in many U.S. regions. A solar-reflective roof is typically light in color and absorbs less sunlight than a conventional dark-colored roof. Less absorbed sun light means a lower surface temperature, directly reducing heat gain from the roof and air-conditioning demand. Typical albedo values for low- and high-albedo roofs can be obtained from the cool roofing materials database (CRMD 2007). The albedo of typical standard roofing materials ranges from 0.10–0.25; one can conservatively assume that the average albedo of existing roofs does not exceed 0.20. The albedo of these surfaces can be increased to about 0.55 to 0.60.

For the sloped-roof residential sector, available highly reflective materials are scarce. White asphalt shingles are available, but have a relatively low albedo of about 0.25. Although it can be argued that white coatings can be applied to shingles or tiles to obtain an aged albedo of about 0.5, this practice is not followed in the field. Some highly reflective white shingles are being developed, but are only in the prototype stage. Recently, one U.S. manufacturer has developed and marketing cool-colored fiberglass asphalt shingles with a solar reflectance of 0.25. Some reflective tiles and metal roofing products with greater than 50% reflectivity are also available. Conversely, highly reflective materials for the low-slope commercial sector are on the market. White acrylic, elastomeric and cementatious coatings, as well as white thermoplastic membranes, can now be applied to built-up roofs to achieve an aged solar-reflectance of 0.6.

Table 2 Albedo modification scenarios

Surface-type	Albedo change		
	High	Low	This study
Residential roofs	0.3	0.1	0.25
Commercial roofs	0.4	0.2	0.25
Pavements	0.25	0.15	0.15

Source: Akbari et al. (2003)

Pomerantz et al. (1997, 2000a, b) and Pomerantz and Akbari (1998) have documented the solar reflectance of many standard and reflective paved surfaces including paving materials such as chip seal, slurry coating, light-color coating. They report that the solar reflectance of a freshly installed asphalt pavement is about 0.05. Aged asphalt pavements have a solar reflectance between 0.10–0.18, depending on the type of aggregate used in the asphalt mix. A light-color (low in carbon content) concrete can have an initial solar reflectance of 0.35–0.40 that will age to about 0.25–0.30.

Akbari et al. (2003) provide estimates for two scenarios for potential changes in the albedo of roofs and paved surfaces (See Table 2). Based on these data, we assume that roof albedo can increase by 0.25 for a net change of $0.25 \times 0.25 = 0.06$. The pavement albedo can increase by 0.15 for a net change of $0.35 \times 0.15 = 0.04$. Hence, the net potential change in albedo for urban areas is estimated at 0.10. Increasing the albedo of urban areas by 0.1 results in an increase of 3×10^{-4} in the Earth's albedo.

4 Methodology to estimate urban albedo effects on radiative forcing

Changing albedo of urban surfaces and changing atmospheric CO_2 concentrations both result in a change in radiative forcing. In these calculations, using the existing data, we will first estimate the increase in radiative forcing from increasing the atmospheric CO_2 by 1 tonne (Section 5). Then through a simple model, we estimate the decrease in radiative forcing by increasing the albedo of roofs and paved surfaces in the urban areas (Section 6). A simple comparison of these two radiative forcings allows us to relate the changes in the solar reflectance of urban surfaces to the changes in the atmospheric CO_2 content.

We note that there are several underlying assumptions/approximations made in our calculations that may affect the projections of CO_2 offsets from increasing urban albedos, when equating urban albedo effects with that of CO_2 on radiative forcing. These are listed as follows:

1. Any discussion of atmospheric CO_2 involves a time series of physical effects, e.g., sequestration in land or ocean. Here we are interested only in the short-term effect (25–50 years). We ignore any time dependence and economics.
2. Using the existing short-wave radiation balance models for the earth–atmosphere system, our calculations for radiative forcing changes implicitly account for the effect of multiple scattering and absorption of radiation within the atmosphere caused by the increased reflectance from urban surfaces. The calculations are performed for the entire globe combining the effects of clouds and atmospheric scattering and absorption into two components—atmospheric absorption and atmospheric reflection. The cloud cover over the oceans is typically higher than over the land. Meanwhile, the atmospheric absorption over the land in some urban areas may be higher because of increased absorption

of radiation by some aerosol species such as black carbon that may increase the heating within the atmospheric layer, especially in areas where black carbon concentrations are relatively high. The relative effects of these factors are hard to estimate without using a detailed radiative transfer model coupled to a chemical transport model (outside the scope of this work), and may to some extent be offset by the effects of local climate on smog formation. For example it has been shown that reflective surfaces in general result in cooler urban temperatures, in turn slowing the formation of smog and decreasing the urban boundary layer thickness. Observations and simulations of smog concentration versus ambient temperature have also shown that cool urban surfaces have a dramatic effect in reducing urban smog (Taha 2005, 2008a, b). Also, most non-metallic surfaces (independent of their solar reflectance) absorb over 90% of the incoming UV light (Levinson et al. 2005a, b) and thus, we do not expect any UV-related effect on photochemical urban smog because of reflective urban surfaces.

3. In most urban areas, residential and suburban neighborhoods constitute the majority of the surfaces (the fraction of areas with tall buildings are fairly small). A limited analysis for the effect of shading of roofs by trees and adjacent buildings shows that shadows from all sources reduce the annual incidence of sunlight on residential roofs by about 10–25%, depending on tree cover (Levinson et al. 2008). This tends to reduce the equivalent potential of cool surfaces by a similar 10–25%.

5 Radiative forcing from atmospheric CO_2

To estimate the radiative forcing associated with CO_2, we consider four different sources as indicated in Table 3. Hansen et al. (1997a) estimate a $2 \times CO_2$ adjusted top-of-atmosphere (TOA) radiative forcing (RF) of 4.19 W m^{-2}. In a more recent study, Hansen et al. (2005) estimate an adjusted RF of 3.95 ± 0.11 W m^{-2}. This yields a RF of 0.93 kW/tonne of CO_2. Estimates used in the IPCC (2007), are based on Myhre et al. (1998) who use RF [W m^{-2}] $= 5.35 \ln(1 + \Delta C/C) = 5.35 \times \ln(2)$ to obtain a RF of 3.71 W m^{-2}. This yields a RF of 0.88 kW/tonne of CO_2. Also using Myhre's equation and estimating the marginal RF at the current atmospheric concentration of 385 ppmv, we estimate a RF of 0.91 kW/tonne of CO_2 {(5.35/385) [W m^{-2}/ppmv] $\times$ (5.1×10^{14}) [m^2] $\times$ (0.128) [ppmv/Gt] $\times$ (10^{-9}) [Gt/t] $\times$ (10^{-3}) [kW/W]}. In these calculations, we estimate that 1 Gt of CO_2 increases the atmospheric CO_2 concentration by 0.128 ppmv (see Table 3, Note c). Note that the three methods used yield almost similar results; hence, we will use an average of 0.91 kW/tonne of CO_2 for the remainder of these calculations.

When equating the forcing between CO_2 and urban albedo changes, we consider CO_2 that is in the atmosphere at a given time. Hence, we do not explicitly consider the time dimensions for the two forcings (urban albedo change and forcing from CO_2). We also note the approach of Matthews and Caldeira (2008) who attempt to calculate the effective forcing from CO_2 on a decadal to century time scale. Using an earth system model with the carbon cycle, Matthews and Caldeira (2008) found a 0.175°C temperature increase for every 100 GtC emitted and estimate that every 100 GtC is ~5% of the climate sensitivity (3.5°C by $2 \times CO_2$) in the model they use. Thus, they suggest that, on the decadal to century time scale, the effective radiative

Table 3 Radiative forcing at the top of the atmosphere (TOA) and CO_2 equivalence

Row	Item	Value
1a.	$2 \times CO_2$ TOA radiative forcing (RF)—Hansen et al. estimate[a]	3.95 W m^{-2}
1b.	$2 \times CO_2$ TOA radiative forcing (RF)—IPCC estimate[b]	3.70 W m^{-2}
2.	Increase in atmospheric concentration by doubling CO_2	275 ppmv
3.	Increases in atmospheric concentration by adding 1Gt of CO_2[c]	0.128 ppmv
4.	Increase in atmospheric CO_2 by doubling concentration [Row 2/Row 3]	2.15×10^{12} tonne
5.	Surface area of the Earth	5.1×10^{14} m^2
6a.	Total radiative forcing on the Earth [Row 1a × Row 5], Hansen RF	2.01×10^{15} W
6b.	Total radiative forcing on the Earth [Row 1b × Row 5], IPCC RF	1.89×10^{15} W
7a.	TOA radiation change per tonne of *atmospheric* CO_2 [Row 6a/Row 4], Hansen RF	$\approx$ 0.93 kW/tonne CO_2
7b.	TOA radiation change per tonne of *atmospheric* CO_2 [Row 6b/Row 4], IPCC RF	$\approx$ 0.88 kW/tonne CO_2
7c.	Incremental TOA radiation change per tonne of *atmospheric* CO_2 (at current concentration of 385 ppmv) using Myhre equation	$\approx$ 0.91 kW/tonne CO_2
7d.	TOA radiation change per tonne of atmospheric CO_2, average of Row 7a–7c	$\approx$ 0.91 kW/tonne CO_2
7e.	TOA radiation change per tonne of *emitted* CO_2 (long-term) using Caldeira's estimate[d]	$\approx$ 0.26 kW/tonne CO_2

[a]Hansen et al. (2005)

[b]IPCC (2007)

[c]The current atmospheric CO_2 concentration is about 385 ppmv corresponding to about 3,000 Gt CO_2 (Trenberth et al. 1988). At current conditions, we estimate an increase of 385/3,000 = 0.128 ppmv/Gt of CO_2

[d]Matthews and Caldeira (2008). Note that the radiation change is estimated per tonne of *emitted* CO_2

forcing from CO_2 after accounting for carbon cycle effects is ~5% × 3.7 W m^{-2} × 5.1×10^{14} m^2/(100 GtC) = 0.26 kW/tonne of emitted CO_2. Here 3.7 W m^{-2} is the IPCC radiative forcing for $2 \times CO_2$. IPCC (2007) estimates that only 55% of the emitted CO_2 stays in the atmosphere. Then Mathews and Caldeira's estimates of effective radiative forcing is 0.26/0.55 = 0.47 kW/tonne of atmospheric CO_2. This value is considerably lower than the range in RF per tonne of CO_2 obtained prior, but nevertheless indicate how these values may differ depending on the model and assumptions used.

6 The effect of changing urban albedos on global radiative forcing

Hansen et al. (1997a) have estimated an adjusted top of the atmosphere RF of −3.70 W m^{-2} for increasing the albedo of 'Tropicana' by 0.2. We estimate that Tropicana is 22% of the land area (a major portion of land area between 22° S to 30° N and 20°–50° E indicated in Fig. 1 of Hansen et al. (1997b)); or about 1/16th of the global surface. For the reflected surfaces, the radiative forcing per 0.01 increase in albedo as estimated by Hansen et al. (1997a) is −2.92 W m^{-2} of Tropicana land.

This estimate appears to be high. Alternatively, as shown in the left side of Fig. 2, Kiehl and Trenberth (1997) estimate that of the total global average of 342 W m^{-2} incident short-wave solar radiation, 77 W m^{-2} (22.5%) is reflected by the atmosphere (that include clouds, aerosols, and the atmosphere), 67 W m^{-2} (19.6%) is absorbed by the atmosphere (again including clouds, aerosols, and the atmosphere), and 168 W m^{-2} (49.1%) is absorbed by the earth's surface (see Fig. 2). Kiehl and Trenberth also estimate that the reflected radiation at TOA from the surface is 30 W m^{-2} (8.8%) net. All these include the effect of multiple scattering by the earth atmosphere-and-surface system. We use the Kiehl and Trenberth data and a simple single-path model to estimate the sensitivity of RF at TOA to the solar reflectance at the surface.

Let f be the fraction of radiation absorbed by the atmosphere (including the clouds) either for incoming or reflected shortwave radiation. Of the 265 W m^{-2} net (342–77 W m^{-2}) incident shortwave radiation $265f$ W m^{-2} (Term A: absorption of in-coming solar radiation) is absorbed by the atmosphere. The atmospheric absorption of the reflected shortwave radiation from the earth's surface is estimated at $30f/(1-f)$ W m^{-2} (Term B: absorption of reflected solar radiation). The sum of Term A and Term B is equal to total short-wave atmospheric absorption of 67 W m^{-2} (i.e., $265f + 30f/(1-f) = 67$). Solving this quadratic equation yields $f = 22.1\%$. Hence, we estimate an incident short-wave radiation of $265 \times (1-f) =$ 206 W m^{-2} on the surface. This value is within the range (169–219 W m^{-2}) given in Hatzianastassiou et al. (2005) based on estimates from several studies. However, Hatzianastassiou et al. (2005) themselves estimate that only 172 W m^{-2} of short-wave radiation reaches the earth surface. This would require that about 50% of the SW radiation is either absorbed or reflected by the atmosphere. Using a simple scaling, we recalculate $f = 26\%$. Then we calculate a change in RF per 0.01 change in solar

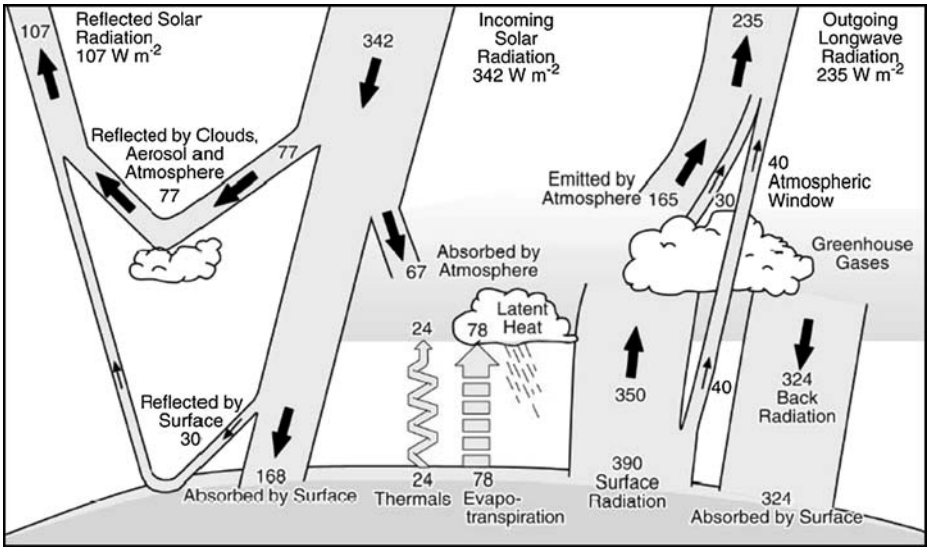

Fig. 2 Schematics of Earth short-wave and long-wave energy balance (source: Kiehl and Trenberth 1997). All numbers are in watts per square meter of earth surface area

Table 4 Radiative forcing of changing roofs and pavements albedo and their equivalent CO_2 offset

Row	Item	Value
1.	Average RF for an albedo increase of 0.01 (see Section 6)	-1.27 W m^{-2}
2.	*Atmospheric* CO_2 equivalent for 0.01 albedo increase of urban area [Row 1/Row 7d Table 3]	-1.40 kg CO_2 m^{-2} of urban area
3.	Fraction of emitted CO_2 that remains in the atmosphere	0.55
4.	*Emitted* CO_2 equivalent offset for 0.01 increase in albedo of urban surface (based on IPCC estimate of RF) [Row 2/Row 3][a]	-2.55 kg CO_2 m^{-2} of urban area
5.	Proposed change in the solar reflectance of roofs	0.25
6a.	*Emitted* CO_2 offset for increasing roof albedo by 0.25	-64 kg CO_2 m^{-2} of roof area
6b.	Cool roof area to offset 1 tonne of emitted CO_2	16 m^2
7.	Proposed change in the solar reflectance of pavements	0.15
8a.	*Emitted* CO_2 offset for increasing pavement albedo by 0.15	-38 kg CO_2 m^{-2} of paved area
8b.	Cool pavement area to offset 1 tonne of emitted CO_2	26 m^2

[a]For comparison, using Matthews and Caldeira's methodology, we estimate an *emitted* CO_2 equivalent offset of -4.90 kg CO_2 m^{-2}

reflectance of the surface to be $(1 - f) \times 172/100 = -1.27$ W m^{-2}. We use this lower estimate for the remainder of our calculations (see Table 4, Row 1).

We note that our calculations apply for the average cloud cover over the earth. The RF for albedo change is a strong function of the cloud cover. The larger the cloud cover, the lower the RF resulting from changes in surface albedo. Thus, depending on the location of urban areas considered, the RF values would need to be adjusted for variations of local cloud cover with respect to the average, which is not considered in our calculations.

Using the estimated kW RF per tonne of atmospheric CO_2 in Table 3, we calculate a CO_2 equivalency of -1.40 kg of CO_2 per m^2 of urban areas for a 0.01 change in albedo (see Table 4, Row 2). IPCC (2007) estimates that only 55% of the emitted CO_2 stays in the atmosphere. Using the IPCC RF equivalent for cool roofs with a proposed albedo change of 0.25, the emitted CO_2 offset is then estimated at -64 kg CO_2 per m^2 of roof area (i.e., 16 m^2 of cool roof area to offset 1 tonne of emitted CO_2).[2] For cool pavements with a proposed albedo change of 0.15, the emitted CO_2 offset is equal to -38 kg CO_2 per m^2 of pavement area (i.e., 26 m^2 of cool paved area to offset 1 tonne of emitted CO_2).

7 Global cooling: CO_2 equivalence

We estimate that urban areas are at least 1% of the Earth's land area or about 1.5×10^{12} m^2 (see Table 5). The roof area is 3.8×10^{11} m^2. The paved surface area is 5.3×10^{11} m^2. We calculate a global RF of -4.4×10^{-2} W m^{-2} by cool roofs and cool pavements. We then estimate the global emitted CO_2 offset potentials for cool roofs and cool pavements to be in the range of 24 Gt of CO_2 and 20 Gt of CO_2, respectively, giving a total global emitted CO_2 offset potential range of 44 Gt of CO_2. This 44 Gt

[2]A cooler roof on a typical new house with a roof area, including garage, of about 180 m^2 offsets the emissions of more than 10 tonnes of CO_2.

Table 5 CO_2 equivalency of increasing the albedo of roofs and pavements in all major hot cities of the world

Row	Item	Value
1.	Area of the earth	510×10^{12} m^2
2.	Land area (29% of Earth area)	147×10^{12} m^2
3.	Dense and developed urban areas (1% of land area)	1.5×10^{12} m^2
4.	Roof area (25% of urban area)	3.8×10^{11} m^2
5.	Paved surface area (35% of urban area)	5.3×10^{11} m^2
6.	Potential emitted CO_2 offset for cool roofs [Row 4 × Row 6a Table 4]	24 Gt CO_2
7.	Potential emitted CO_2 offset for cool pavements [Row 5 × Row 8a Table 4]	20 Gt CO_2
8.	Total potential emitted CO_2 offset for cool roofs and cool pavements [Row 6 + Row 7]	44 Gt CO_2
9.	Projected 2025 world CO_2 emissions[a]	37 Gt CO_2/year

[a]EIA (2003). International Energy Outlook. Energy Information Administration. Washington D.C.

CO_2 offset is over 1 year of the 2025 projected world-wide emission of 37 Gt of CO_2 per year (EIA 2003).

Currently, in Europe emitted CO_2 is traded at ~$25/tonne. For a typical house with a 100 m^2 roof area, the total CO_2 offset is 6 t, worth $150 (an average of about $1.5/m^2). For each 100 m^2 of paved area, the total offset is 4 t CO_2, worth $100 (an average of about $1/m^2). A 44 Gt CO_2 emission offset from changing the albedo of roofs and paved surfaces is worth about $1,100 billion. The contribution of cooler roofs to this CO_2 offset is thus worth $600 billion. However, we note that these offsets are applicable only as long as the solar reflectivities of urban surfaces are maintained.

8 Uncertainties

Several sources of uncertainties can affect the estimates of CO_2 offset resulting from increasing the albedo of urban surfaces:

1. The estimates of radiative forcing for 2 × CO_2 is about 3.7–4.1 W m^{-2} introducing a potential 10% error in our results;
2. As was noted in Section 5, methodologies to account for the long-term effects of atmospheric CO_2 on global warming can potentially increase our estimates by almost a factor of two;
3. We used an average cloud cover for the globe to estimate the RF effect of increasing albedo of urban surfaces. The cloud cover in most urban areas is lower than the average cloud cover of the earth. This would increase the RF effect of reflective surfaces;
4. In our analysis, we have estimated that available urban surfaces for potential increase of their albedo are about 1% of the land surface of the earth. Any under- or over-estimation in this estimate directly scales our results.

Considering all these factors, we estimate that the global potential for increasing albedo of urban areas can range from 30 Gt to about 100 Gt of CO_2.

9 Conclusions

Using cool roofs and cool pavements in urban areas, on an average, can increase the albedo of urban areas by 0.1. We estimate that increasing the albedo of urban roofs and paved surfaces will induce a negative radiative forcing of 4.4×10^{-2} W m^{-2} equivalent to offsetting 44 Gt of emitted CO_2. A 44 Gt of emitted CO_2 offset resulting from changing the albedo of roofs and paved surfaces is worth about $1,100 billion. Assuming a plausible growth rate of 1.5% in the world's CO_2-equivalent emission rate, we estimate that the 44 Gt CO_2-equivalent offset potential for cool roofs and cool pavements would counteract the effect of the growth in CO_2-equivalent emission rates for 11 years.

We emphasize that these calculations and estimates are preliminary in nature. Converting to cool urban surfaces does not address the underlying problem of global warming, which results from the emissions of greenhouse gases and absorbing particles. The problem of global warming emissions must be resolved by developing and implementing a complete portfolio of measures to reduce GHG emissions. We also note that the cool urban surfaces, particularly cool roofs, yield significant energy savings and hence a reduction in GHG emissions. The global cooling effect of increasing urban solar reflectance is an added effect that is quantified here.

Acknowledgements This work was supported by the California Energy Commission (CEC) through its Public Interest Energy Research Program (PIER) and by the Assistant Secretary for Energy Efficiency and Renewable Energy under Contract No. DE-AC02-05CH11231. We thank Dr. Ken Caldeira for enlightening us about radiative forcing and Dr. M. MacCracken for extensive comments and discussions. Additional thoughtful comments from G. Franco, M. Jacobson, and J. Sathaye helped improve this paper. R. Levinson helped us with the analysis of urban areas, using the GRUMP (Urban Extension) data.

References

Akbari H, Rose LS (2001a) Characterizing the fabric of the urban environment: a case study of metropolitan Chicago, Illinois. Lawrence Berkeley National Laboratory Report LBNL-49275, Berkeley, CA

Akbari H, Rose LS (2001b) Characterizing the fabric of the urban environment: a case study of Salt Lake City, Utah. Lawrence Berkeley National Laboratory Report No. LBNL-47851, Berkeley, CA

Akbari H, Konopacki S (2005) Calculating energy-saving potentials of heat-island reduction strategies. Energy Policy 33:721–756

Akbari H, Pomerantz M, Taha H (2001) Cool surfaces and shade trees to reduce energy use and improve air quality in urban areas. Sol Energy 70(3):295–310

Akbari H, Rose LS, Taha H (2003) Analyzing the land cover of an urban environment using high-resolution orthophotos. Landsc Urban Plan 63:1–14

Balk D, Pozzi F, Yetman G, Deichmann U, Nelson A (2004) The distribution of people and the dimension of place: methodologies to improve the global estimation of urban extents. Online at http://sedac.ciesin.columbia.edu/gpw/docs/UR_paper_webdraft1.pdf

CIESIN (2007) Gridded population of the world and the global rural–urban mapping project. Center for International Earth Science Information Network, Earth Institute, Columbia University. Online at http://sedac.ciesin.columbia.edu/gpw/

CRMD (2007) Cool roof material database. http://eetd.lbl.gov/CoolRoofs/

Demographia (2007) Demographia world urban areas projections 2007 & 2020 (World Agglomerations). Demographia, PO Box 841, Belleville, Illinois 62222 USA

EIA (2003) International energy outlook. Energy Information Administration, Washington D.C.

Hansen J, Sato M, Ruedy R (1997a) Radiative forcing and climate response. J Geophys Res 102(D6):6831–6864
Hansen J, Ruedy R, Lacis A, Russell G, Sato M, Lerner J, Rind D, Stone P (1997b) Wonderland climate model. J Geophys Res 102(D6):6823–6830
Hansen J, Sato M, Ruedy R et al. (2005) Efficacy of climate forcing. J Geophys Res 110:D18104
Hatzianastassiou N, Matsoukas C, Fotiadi A, Pavlakis KG, Drakakis E, Hatzidimitriou D, Vardavas I (2005) Global distribution of Earth's surface shortwave radiation budget. Atmos Chem Phys 5:2847–2867
IPCC (2007) Climate change 2007—the physical science basis, contribution of working group I to the fourth assessment report of the IPCC. Chapter 7, Figure 7.4 and Section 7.3.2.1 (516–517)
Kiehl JT, Trenberth KE (1997) Earth's annual global mean energy budget. Bull Am Meteorol Soc 78(2):197–208, February
Levinson R, Berdahl P, Akbari H (2005a) Solar spectral optical properties of pigments, part I: model for deriving scattering and absorption coefficients from transmittance and reflectance measurements. Sol Energy Mater Solar Cells 89(4):319–349
Levinson R, Berdahl P, Akbari H (2005b) Solar spectral optical properties of pigments, part II: survey of common colorants. Sol Energy Mater Sol Cells 89(4):351–389
Levinson R, Akbari H, Pomerantz M, Gupta S (2008) Estimating the solar access of typical residential rooftops: a case study in San Jose, CA. Solar 2008. American Solar Energy Society, San Diego CA, May 3–5
Matthews HD, Caldeira K (2008) Stabilizing climate requires near-zero emissions. Geophys Res Lett 35:L04705
McGranahan G, Marcotullio P, Bai X, Balk D, Braga T, Douglas I, Elmquist T, Rees W, Satterthwaite D, Songsore J, Zlotnik H (2005) Urban systems. In: Hassan R, Scholes R, Ash N (eds) Chapter 27 in ecosystems and human well-being: current state and trends. Island Press, Washington, DC, pp 795–825, http://www.maweb.org/documents/document.296.aspx.pdf
Myhre et al. (1998) New estimates of radiative forcing due to well-mixed greenhouse gases. Geophys Res Let 25(14):2715–2718
Pomerantz M, Akbari H (1998) Cooler paving materials for heat island mitigation. In: Proceedings of the 1998 ACEEE summer study on energy efficiency in buildings, vol 9, p 135
Pomerantz M, Akbari H, Berdahl P, Konopacki SJ, Taha H (1999) Reflective surfaces for cooler buildings and cities. Philos Mag B 79(9):1457–1476
Pomerantz M, Akbari H, Chen A, Taha H, Rosenfeld AH (1997) Paving materials for heat island mitigation. Lawrence Berkeley National Laboratory Report No. LBL-38074, Berkeley, CA
Pomerantz M, Akbari H, Harvey JT (2000a) The benefits of cooler pavements on durability and visibility. Lawrence Berkeley National Laboratory Report No. LBNL-43443, Berkeley, CA
Pomerantz M, Pon B, Akbari H, Chang S-C (2000b) The effect of pavement temperatures on air temperatures in large cities. Lawrence Berkeley National Laboratory Report No. LBNL-43442, Berkeley, CA
Rose LS, Akbari H, Taha H (2003) Characterizing the fabric of the urban environment: a case study of Greater Houston, Texas. Lawrence Berkeley National Laboratory Report LBNL-51448, Berkeley, CA
Rosenfeld AH, Romm JJ, Akbari H, Pomerantz M (1998) Cool communities: strategies for heat islands mitigation and smog reduction. Energy Build 28(1):51–62
Taha H (2001) Potential impacts of climate change on tropospheric ozone in California: a preliminary episodic modeling assessment of the Los Angeles Basin and the Sacramento Valley. Lawrence Berkeley National Laboratory Report No. LBNL-46695, Berkeley, CA
Taha H (2002) Meteorological and air quality impacts of increased urban surface albedo and vegetative cover in the Greater Toronto Area, Canada. Lawrence Berkeley National Laboratory Report No. LBNL-49210, Berkeley, CA
Taha H (2005) Surface modifications as a potential ozone air-quality improvement strategy in California: Part I: mesoscale modeling. Final report prepared for the California Energy Commission; available from the CEC website at: http://www.energy.ca.gov/2005publications/CEC-500-2005-128/CEC-500-2005-128.PDF
Taha H (2008a) Episodic performance and sensitivity of the urbanized MM5 (uMM5) to perturbations in surface properties in Houston TX. Boundary-Layer Meteorol 127:193–218. doi:10.1007/s10546-007-9258-6
Taha H (2008b) Urban surface modification as a potential ozone air-quality improvement strategy in California: a mesoscale modeling study. Boundary-Layer Meteorol 127:219–239. doi:10.1007/s10546-007-9259-5

Taha H, Chang S-C, Akbari H (2000) Meteorological and air quality impacts of heat island mitigation measures in three U.S. Cities. Lawrence Berkeley National Laboratory Report No. LBL-44222, Berkeley, CA

Trenberth KE, Christy JR, Olson JG (1988) Global atmospheric mass, surface pressure, and water vapor variations. J Geophys Res 93(D9):10,925

USGS (1999) United States Geological Survey (USGS)/University of Nebraska, Lincoln/European Commission joint research center 1-km resolution global land cover characteristics database, derived from advanced very high resolution radiometer (AVHRR) data from the period April 1992 to March 1993